The Reaction of n - and i -C 4 H 5 Radicals with Acetylene †

ARTICLE *in* THE JOURNAL OF PHYSICAL CHEMISTRY A · JUNE 2007

Impact Factor: 2.69 · DOI: 10.1021/jp0675126 · Source: PubMed

2 AUTHORS, INCLUDING:

Juan Pablo Senosiain
Laboratorios Senosiain
18 PUBLICATIONS **596** CITATIONS

SEE PROFILE

The Reaction of *n*- and *i*-C_4H_5 Radicals with Acetylene†

Juan P. Senosiain*,‡ and James A. Miller§

Departamento de Química Física, Facultade de Química, Universidade de Santiago de Compostela, Avda. das Ciencias s/n, Santiago de Compostela 15782, Spain, and Combustion Research Facility, Sandia National Laboratories, Livermore, California 94551-0969 MS 9055

Received: November 13, 2006; In Final Form: March 1, 2007

In this article, we discuss the reactions of *i*-C_4H_5 and *n*-C_4H_5 with acetylene. Both have been proposed as possible cyclization steps, forming benzene or fulvene, in rich flames burning aliphatic fuels. The relevant parts of the potential energy surface were determined from rQCISD(T) calculations extrapolated to the infinite-basis-set limit. Using this information in a Rice−Ramsperger−Kassel−Marcus-based master equation, we have calculated thermal rate coefficients and product distributions for both reactions as a function of temperature and pressure. The results are cast in forms that can be used in modeling, and the implications of the results for flame chemistry are discussed.

I. Introduction

Perhaps the most challenging problem in gas-phase combustion chemistry is the quantitative prediction of the concentrations of aromatic compounds, polycyclic aromatic hydrocarbons (PAH), and their precursors in flames burning aliphatic fuels. This topic has long been of interest because of its connection with soot formation, but interest in it has increased since the Clean Air Act amendments of 1990 in the United States which regulated emissions of many such compounds from industrial banners, calling them "air toxic species". Examples of air toxics include benzene, toluene, and 1,3-butadiene, among other species that commonly accompany PAH formation under rich combustion conditions. The accurate modeling of such species in flames requires dealing with a degree of complexity not encountered in other combustion problems. Consequently, many of the important issues are only beginning to take focus, and relatively few have been resolved satisfactorily.

Current conventional wisdom has it that PAH and soot are formed from a "first ring", probably benzene or phenyl, but perhaps from some other six-membered ring.[1−4] This first ring serves as the nucleus for the formation of PAH, perhaps by a mechanism that involves sequentially adding acetylene molecules. At a molecular weight of about 2000 amu, it becomes easier to think of the PAHs as solid particles rather than molecules. These are the earliest soot particles, although they undergo considerable physical and chemical transformations before they look like the soot particles that are emitted from practical combustors.

Clearly, the formation of the first ring is a critical part of this process. It has even been conjectured that this step may control the overall rate of PAH and soot formation,[5,6] at least under some conditions. As a result, a significant amount of effort has been devoted to understanding how the first ring is formed. It is now reasonably well-established that resonantly stabilized free radicals (RSFRs) play a key role not only in the formation of the first ring but perhaps also in the growth of larger PAH.[1−4,7] The increased thermal stability that resonance stabilization affords a free radical allows RSFRs to grow to fairly large concentrations in flames. The reactions between two RSFRs are particularly attractive as cyclization steps, because the deeper potential energy wells of the initial adducts in radical−radical reactions are more likely to support the molecular rearrangement required for cyclization to occur than are the corresponding wells for radical−molecule reactions. Currently, we believe that $C_3H_3 + C_3H_3$, where C_3H_3 is propargyl, is the dominant cyclization step under the vast majority of combustion conditions, probably with contributions from $C_3H_3 + C_3H_5$, where C_3H_5 is allyl, in some instances.

Miller and Melius[8] suggested that there was at least one radical−molecule reaction that could break the "radical−radical rule" and lead effectively to cyclic species. That reaction is the one between *i*-C_4H_5 and acetylene. Recent measurements in flames[9] indicate that virtually all of the C_4H_5 present is either *i*-C_4H_5 (CH_2CHCCH_2) or one of two methyl-substituted propargyl radicals (CH_3CCCH_2 or $CHCCHCH_3$). All three are resonantly stabilized. The nonresonantly stabilized *n*-C_4H_5 isomer ($CH_2CHCHCH$) was not detected, primarily because of low concentrations, but also because of low sensitivity in the experiments. CH_3CCCH_2 and $CHCCHCH_3$ can be formed from the reaction of methyl with propargyl

$$CH_3 + C_3H_3 \rightarrow CH_3CCCH_2 + H$$

$$CH_3 + C_3H_3 \rightarrow CHCCHCH_3 + H$$

by simple exchange reactions. These radicals could lead to cyclization by reacting with propargyl, with themselves, or with each other, forming methyl-substituted benzene molecules (toluene, ortho-xylene, etc.), by mechanisms analogous to that of the $C_3H_3 + C_3H_3$ reaction.[10] However, that is a subject for another time.

The present article concerns itself primarily with a rigorous theoretical treatment of the *i*-C_4H_5 + acetylene reaction, providing rate coefficients that can be used with some confidence in flame modeling to assess the importance of the reaction as a cyclization step. We also include a similar treatment of the

† Part of the special issue "James A. Miller Festschrift".

* Corresponding author. E-mail: jpsenosiain@gmail.com. Phone: +34 981563100 ext.14303.

‡ Universidade de Santiago de Compostela.

§ Sandia National Laboratories.

10.1021/jp0675126 CCC: $37.00
Published on Web 04/05/2007

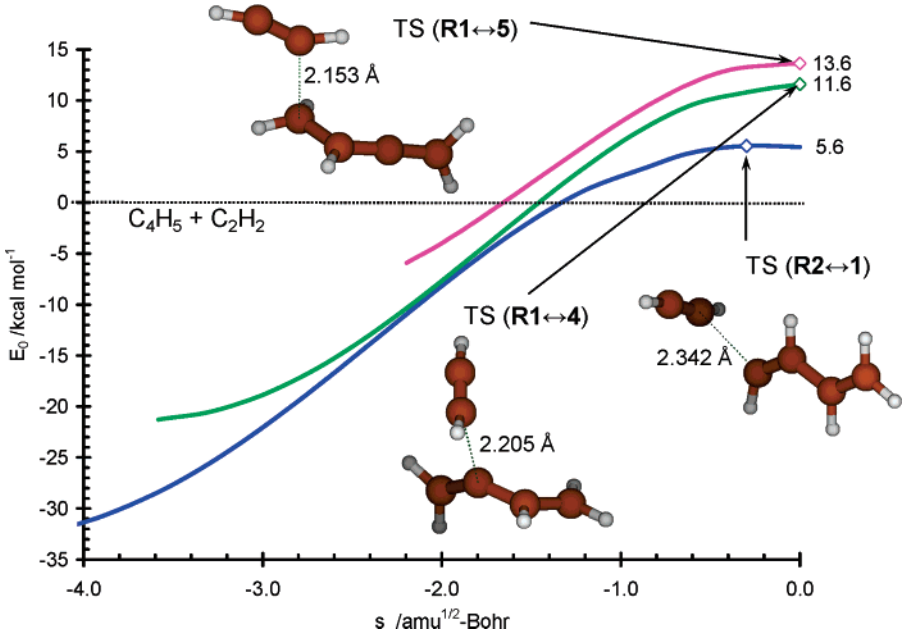

Figure 1. Addition potentials (including ZPE) for acetylene addition to *n*- and *i*-C_4H_5 radicals, calculated at the rQCISD(T)/cc-pV∞Z//uB3LYP/6-311++G(d,p) level of theory (see text for details).

n-C_4H_5 + C_2H_2 reaction, primarily for comparison purposes. However, the latter reaction cannot be ruled out completely as a minor contributor to benzene formation in low-temperature zones of combustors, where it can be formed from the reaction of vinyl with acetylene.[11] In such low-temperature zones, hydrogen atoms may not be present in sufficient quantities to catalyze its conversion to *i*-C_4H_5,

$$n\text{-}C_4H_5 + H \rightarrow i\text{-}C_4H_5 + H$$

To our knowledge, there is no direct experimental information available on either of the title reactions.

II. Computational Details

A. Theoretical Model Chemistries. The B3LYP[12,13] hybrid density functional theory (DFT) method was employed, together with Pople's split-valence 6-311++G(d,p) basis set, to optimize the geometries and compute the vibrational frequencies of all complexes and (first-order) saddlepoints. Additionally, we calculated rotational potentials for species with internal rotations, intrinsic reaction coordinate (IRC) curves, and projected vibrational frequencies[14] along these curves for the association channels, using this theoretical model chemistry. In order to obtain accurate reaction energy barriers, we carried out further single-point energy calculations at these geometries using Dunning's basis sets, cc-pV*x*Z, with $x = \{T,Q\}$ and two different treatments of electron correlation. First, we used the spin-restricted quadratic-configuration-interaction[15] with a perturbative estimate of the disconnected triples interactions, rQCISD(T), using a triple-ζ basis set. Then, we performed further calculations using the spin-restricted Møller-Plesset second-order perturbation theory,[16] rMP2, with triple and quadruple-ζ basis sets. Finally, we used the rMP2 energies to correct the rQCISD(T) values for the finite basis set, using the following empirical ansatz:[17]

$$E^{\infty}_{\mathrm{rQCISD(T)}} \approx E^{\mathrm{VTZ}}_{\mathrm{rQCISD(T)}} + \frac{625E^{\mathrm{VQZ}}_{\mathrm{rMP2}} - 256E^{\mathrm{VTZ}}_{\mathrm{rMP2}}}{369} - E^{\mathrm{VTZ}}_{\mathrm{rMP2}} \quad (1)$$

The related rCCSD(T) method has been shown[18] to achieve "chemical accuracy", even in situations where spin contamination would normally be a problem. Although the rQCISD(T) method recovers somewhat less electron correlation, our own unpublished calculations[19] show that energy barriers obtained with the rQCISD(T) method are slightly better than those computed with rCCSD(T) and are accurate to within 1 kcal/mol in most cases. It is well-known that spin-restricted wavefunctions incur considerable error when they are used to calculate systems with geometries far from the equilibrium configurations. However, in many cases including stable complexes and tight transition states, the error introduced by the spin restriction is usually less than that due to spin contamination, which affects methods based on a uHF wavefunction.

The Gaussian 03[20] quantum chemistry package was used for the calculation of optimized geometries, vibrational frequencies, and IRCs. Single-point energy calculations were performed using the Molpro[21] electronic structure package. All calculations were performed with an eight-core server running Linux.

B. Master Equation Model. The rate coefficients as a function of pressure and temperature were computed by solving the one-dimensional master equation (ME), that is, resolved in terms of the total energy,

$$\frac{dn_i(E)}{dt} = Z\int_{E_{0_i}}^{\infty} P(E \leftarrow E')n_i(E')dE' - Zn_i(E) - \sum_{j\neq i}^{N_{\mathrm{wells}}} k_{ji}(E)n_i(E) + \sum_{j\neq i}^{N_{\mathrm{wells}}} k_{ij}(E)n_j(E) - \sum_{\alpha}^{N_{\mathrm{prod}}} k_{\mathbf{P}_\alpha i}(E)n_i(E) + n_{\mathbf{R}}K^{\mathrm{eq}}_{\mathbf{R}i}k_{\mathbf{R}i}(E)\frac{\rho_i(E)e^{-\beta E}}{Q_i(T)} - k_{\mathbf{R}i}(E)n_i(E) \quad (2)$$

where *i* corresponds to a stable complex, **R** corresponds to the reactants, and $\mathbf{P}_\alpha$ corresponds to a set of bimolecular products, as shown in Figure 2. The quantity $n_i(E)$ is the population of complex *i* at energy *E*; E_{0_i} is the ground state energy of complex *i*, and $K^{\mathrm{eq}}_{\mathbf{R}i}$ is the pseudo-first-order equilibrium constant be-

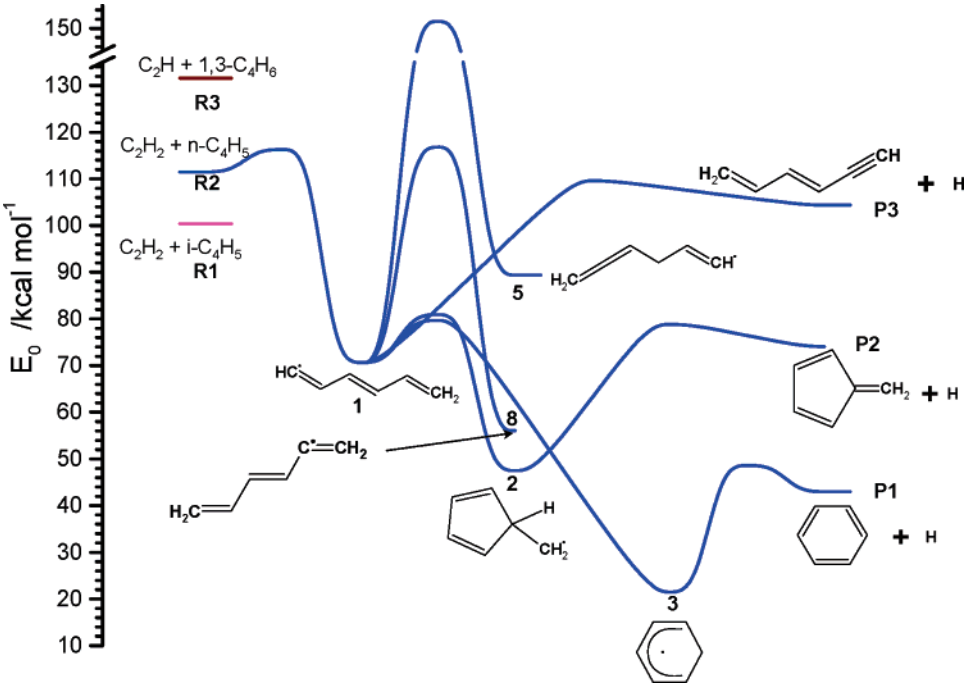

Figure 2. Potential energy diagram for acetylene addition to *n*-C_4H_5 radicals, calculated at the rQCISD(T)/cc-pV∞Z//uB3LYP/6-311++G(d,p) level of theory (see text for details).

tween **R** and complex *i* (i.e., the equilibrium constant multiplied by the concentration of the excess reactant).

The $k_{ji}(E)$ are (microcanonical) isomerization rate coefficients from *i* to *j*, where *i*,*j* are stable isomers on the potential energy surface. Similarly, $k_{\mathbf{P}_\alpha i}(E)$ and $k_{\mathbf{R}i}(E)$ are dissociation rate coefficients from *i* to a set of bimolecular products $\mathbf{P}_\alpha$ and to reactants **R**, respectively. Microcanonical rate coefficients were first computed as functions of total energy and total angular momentum, for example, $k_{ji}(E,J)$, then summed over a sufficient number of *J* values to obtain $k_{ji}(E)$. The rigid-rotor/harmonic-oscillator approximation was assumed in the calculation of energy levels, and the RRKM approximation is inherent in the microcanonical rate coefficients. We used the exact counting method to compute densities and cumulative numbers of states. To compute the density and number of states of internal rotational modes, we used a Pitzer−Gwinn-like approximation.[22] For this purpose, we carried out rotational scans and fit the calculated potentials to a Fourier series, as described elsewhere.[23] Parameters for these fits are provided in Supporting Information for reference. The coupling between internal rotations in species with more than one torsional mode was neglected. One-dimensional tunneling and nonclassical reflection were included using an asymmetric Eckart potential energy function. Association channels were treated variationally, and no adjustments were made to the computed energy barriers because of the lack of reliable experimental data.

In eq 2, *Z* is the collision number per unit time, which is calculated based on a Lennard−Jones potential using parameters of benzene[24] to represent the complexes. Inelastic collisions with a third-body result in an energy transfer incorporated in eq 2 as $P(E \leftarrow E')$, which is the probability that a complex with an energy between E' and $E' + dE'$ will be transferred by a collision to a state with an energy between *E* and $E+dE$. The rates of deactivating collisions were modeled using the "single exponential down" expression:

$$P(E \leftarrow E') \propto \exp\left(-\frac{E'-E}{\langle \Delta E_d \rangle}\right) \qquad E' > E \qquad (3)$$

SCHEME 1: Electronic Resonance Structures of Iso-C_4H_5 Radicals

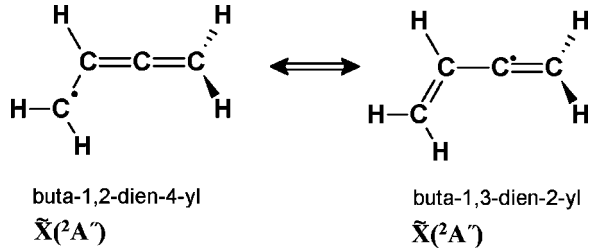

buta-1,2-dien-4-yl $\tilde{X}(^2A'')$ buta-1,3-dien-2-yl $\tilde{X}(^2A'')$

where $\langle \Delta E_d \rangle$ is an energy transfer parameter that depends upon the nature of the collider gas, in this case N_2. We employed a value of $\langle \Delta E_d \rangle = 400\ cm^{-1}(T/300\ K)^{0.7}$ for all complexes. The room-temperature value of this expression is consistent with the experimentally determined[25] $\langle \Delta E \rangle$ for toluene relaxation, and the temperature dependence is similar to that found by Miller and Klippenstein[7] to fit falloff curves for methane dissociation. Collisional energy transfer rates for activating collisions were obtained from detailed balance. Dissociation to bimolecular products was treated irreversibly. Rate coefficients were extracted from the solution eigenpairs following procedures described elsewhere.[10,11,26−29] All rate coefficients were calculated with the VARIFLEX code.[30]

III. Results and Discussion

A. Potential Energy Calculations. The *i*-C_4H_5 radicals belong to the C_s point-group, and their ground-state wavefunction has $^2A''$ symmetry. They are stabilized by the two electronic resonance structures, shown in Scheme 1. According to our calculations, the iso form is 10.5 kcal/mol more stable than the normal isomers. This value agrees very well with that resulting from the focal-point analysis of Wheeler et al.,[31] which is somewhat smaller than that obtained from the earlier G2-like calculations of Miller et al.[11] There are two possible addition sites in *i*-C_4H_5 due to the existence of two electronic resonant structures, shown in Scheme 1. The addition of acetylene to *n*-

TABLE 1: Calculated Energies, Zero-Point Energies, Q1 Diagnostic and $\langle S^2 \rangle$ Values of C_6H_7 Isomers and Several Bimolecular Products

		6-311++G(d,p)			VTZ			VQZ	
species		ZPE[a]	E_0[a]	$\langle S^2 \rangle$[a]	E_0[b]	E_0[c]	Q1 diag[c,d]	E_0[c]	E_0[f]
ref	C_2H_2 + 1,3-C_4H_6−H		0.0		0.0	0.0		0.0	0.0
R1	*i*-C_4H_5 + C_2H_2	60.8	94.3	0.776	98.8	99.3	0.023	99.4	100.4
R2	*n*-C_4H_5 + C_2H_2	61.4	108.0	0.764	109.5	109.3	0.015	110.5	110.9
R3	C_2H + 1,3-C_4H_6	61.9	132.1	0.773	130.8	129.6	0.016	132.0	131.6
1	$CH_2CHCHCHCHCH$	65.4	68.1	0.768	68.7	69.0	0.014	69.7	70.7
2	$CH_2(CHCHCHCHCH)$	66.2	50.7	0.754	41.5	46.3	0.012	42.2	47.5
3	$(CH_2CHCHCHCHCH)$	67.9	21.6	1.497	15.3	20.8	0.016	15.8	21.5
4	(3*E*,4*Z*)-$CH_2CHC(CH_2)CHCH$	65.3	74.3	0.762	72.5	72.7		73.4	74.3
4'[g]	(3*Z*,4*E*)-$CH_2CHC(CH_2)CHCH$	65.2	73.0	0.764	71.4	71.5	0.014	72.4	73.1
5	CH_2CCHCH_2CHCH	64.8	86.7	0.760	88.1	87.7	0.014	89.1	89.4
6	(CH_2CHCCH_2CHCH)	68.1	58.0	0.759	52.1	53.9	0.014	52.9	55.1
7	$CH_2(CCHCH_2CHCH)$	66.9	32.1	0.784	27.1	30.3	0.023	27.7	31.3
8[g]	$CH_2CCHCHCHCH_2$	65.1	50.4	0.789	53.5	55.0	0.018	54.2	56.1
P1[g]	H + C_6H_6	62.8	44.0	0.750	28.9	41.7	0.000	29.6	43.0
P2[g]	H + $CH_2(CCHCHCHCH)$	61.2	77.5	0.750	64.1	72.8	0.000	64.8	74.1
P3[g]	H + $CHCCHCHCHCH_2$	59.2	103.6	0.750	95.3	102.7	0.000	96.3	104.4
P4[g]	H + $CHCC(CH_2)CHCH_2$	59.2	107.1	0.750	96.2	103.8	0.000	97.2	105.3
P5[g]	H + $CHCCH_2CHCCH_2$	58.6	121.4	0.750	113.8	120.4	0.000	114.7	121.8
R2↔1		61.9	113.8	0.776	114.3	114.9	0.016	115.2	116.3
R1↔4		61.8	108.6	0.787	108.5	110.9	0.019	109.1	112.0
R1↔5		61.8	108.7	0.785	110.0	113.0	0.018	110.6	114.0
1↔2		64.8	80.0	0.785	79.5	79.5	0.020	80.3	80.9
1↔3		65.3	78.0	0.783	76.9	78.3	0.017	77.8	79.7
1↔5		61.1	147.8	0.773	148.2	150.1	0.017	149.0	151.5
1↔8		61.0	109.7	0.797	112.0	116.0	0.021	112.5	116.8
1↔P3		60.0	107.7	0.762	102.2	108.4	0.014	102.9	109.6
2↔P2		61.8	81.5	0.781	70.7	78.0	0.015	71.1	78.8
3↔6		64.7	97.1	0.763	90.4	95.7	0.019	90.7	96.1
3↔P1		63.8	47.6	0.769	36.6	47.7	0.014	37.2	48.6
4↔4'	treated as HR	64.9	76.4	0.760	74.4	74.5	0.014	75.4	76.2
4↔P4		59.9	111.8	0.768	103.9	110.1	0.014	104.5	111.2
4'↔7		64.8	84.2	0.793	83.7	83.9		84.6	85.3
5↔6		64.7	96.2	0.781	96.9	96.3	0.019	97.6	97.4
5↔7		64.1	89.6	0.778	90.7	90.3	0.018	91.5	91.6
5↔P5		59.4	124.9	0.761	120.0	125.5	0.014	120.7	126.6
7↔P2		61.7	78.3	0.765	66.5	74.7	0.013	67.0	75.6

[a] uB3LYP/6-311++G(d,p) theory. Units are kcal/mol. [b] rMP2/cc-pVTZ theory. Units are kcal/mol. [c] rQCISD(T)/cc-pVTZ theory. Units are kcal/mol. [d] Q1diagnostic, see refs 34 and 35. [e] rMP2/cc-pVQZ theory. Units are kcal/mol. [f] Calculated with eq 1, see text for details. [g] Not used in the calculations of the rate coefficients.

and *i*-C_4H_5 radicals is characterized by a (first order) saddlepoint on the uB3LYP surface. Figure 1 shows the potential energy relative to the fragments for each addition process. This was calculated with eq 1 and is based on IRC geometries calculated with the uB3LYP/6-311++G(d,p) theory. These potentials include the contribution to the zero-point energy of all modes perpendicular to the reaction coordinate, computed with projected vibrational frequencies.[14] In the case of the *n*-C_4H_5 radical, the maximum of this potential[32] occurs slightly later than the saddlepoint on the uB3LYP surface, but in general, the position of the saddlepoints of the two levels of theory coincide.[33] The calculated barriers for addition to the secondary and primary C atoms of *i*-C_4H_5 radicals are 11.6 and 13.6 kcal/mol, respectively. These values are significantly higher than the barrier for acetylene addition to *n*-C_4H_5 radicals (5.6 kcal/mol), a fact which reflects the energy cost of breaking the electronic resonance in the transition state. Complexes **1**, **4**, and **5** are more stable than the fragments by 40.9, 26.1, and 11.0 kcal/mol, respectively. As expected by Hammond's postulate, the C−C distances between the C_2H_2 and the C_4H_5 moieties of the addition saddlepoints (2.342, 2.205, and 2.153 Å, respectively) increase with the depth of the well, which correspond to structures earlier in the reaction.

The calculated energies of complexes and (first-order) saddlepoints are given in Table 1, along with the zero-point energies, and indicators of spin-contamination and multireference character. Since the optimizations were performed using a spin-unrestricted method, these are prone to spin contamination. However, DFT methods are generally less affected by this issue than the popular MP2 method. A glance at the values of $\langle S^2 \rangle$ listed in Table 1 reveals that only three cases have expectation values higher than 0.79 (all of them are doublets) and only one case (complex **3**) is severely affected by spin contamination, with a value of 1.497. A comparison of the energies calculated with different methods shows that the RMP2 energies differ significantly from those obtained with eq 1, with a root mean square (rms) deviation of 0.88 kcal/mol (for the cc-pVQZ basis set) and absolute deviations as large as 13.2 kcal/mol in some instances. In contrast, the DFT method employed has an rms deviation of 0.46 kcal/mol and has a maximum absolute deviation of 7.2 kcal/mol, and it is not as overbinding as RMP2. However, we note that the RMP2 energies were only used to approximate the difference between the correlation energy of the complete basis set limit and that recovered with the cc-pVTZ basis set. In all cases, the magnitude of these corrections is smaller than 2 kcal/mol. The Q1 diagnostic developed by Lee and co-workers[34,35] gives an indication of the quality of the QCISD wavefunction and the suitability of a wave function based on a single-determinant. All structures listed in Table 1

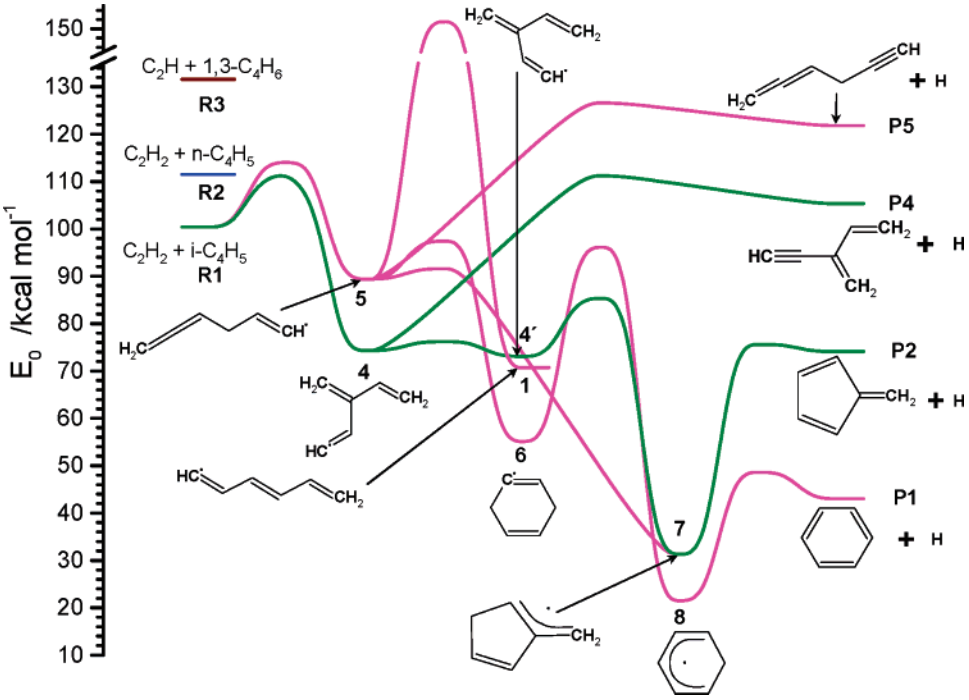

Figure 3. Potential energy diagram for acetylene addition to i-C_4H_5 radicals, calculated at the rQCISD(T)/cc-pV∞Z//uB3LYP/6-311++G(d,p) level of theory (see text for details).

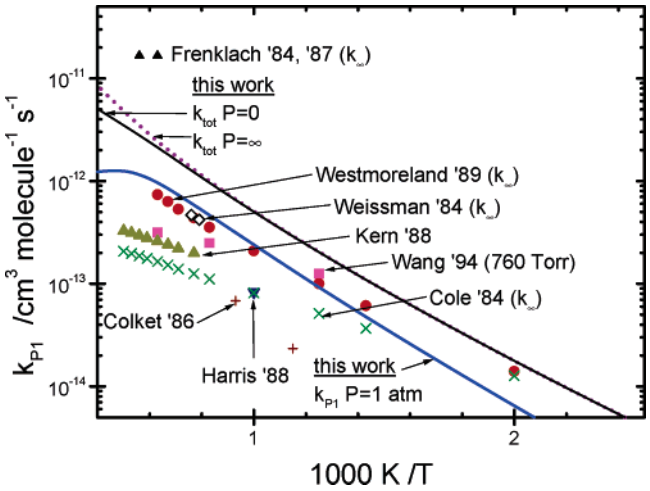

Figure 4. Arrhenius plot for the n-$C_4H_5 + C_2H_2$ reaction. Experimental data for the total rate coefficient[36,38,39,43] and the H + benzene channel[40−42,46] are shown with symbols. Our calculations for 760 Torr of N_2, the collisionless (k_0), and high-pressure (k_∞) limits are shown with thick solid, thin solid, and dotted lines, respectively.

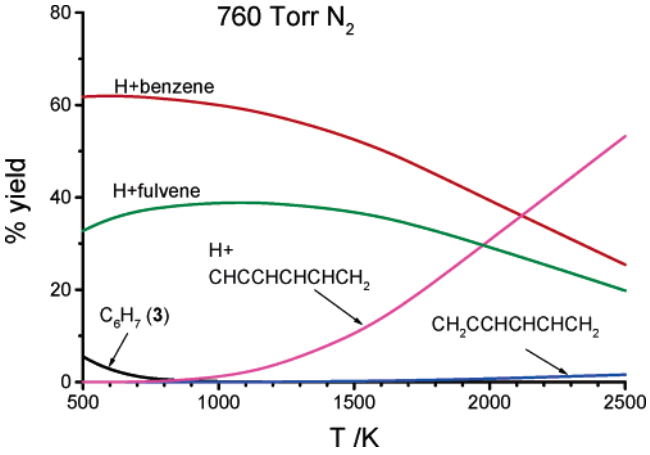

Figure 5. Product yields for the reaction of n-C_4H_5 with acetylene, calculated with 1 atm of N_2 bath gas.

have Q1 values close to or less than 0.02, and so the use of a single-reference method is acceptable.

The relevant points on the potential energy surface for the reaction of n-C_4H_5 with acetylene are shown in Figure 2. These energies are calculated with eq 1 and include zero-point energy, taking C_2H_2 + 1,3-butadiene − H as the reference. For illustration purposes, the potential energy of C_2H_2 + i-C_4H_5 and C_2H + 1,3-C_4H_6, calculated at the same level of theory, are also shown in Figure 2. Energy barriers for forming five- and six-membered rings from **1** (10.3 and 9.1 kcal/mol, respectively) are small compared to the chemical activation of 40.9 kcal/mol of the complex. Thus, under most conditions, complex **1** will close into a ring and dissociate to bimolecular products, with the route leading to benzene being favored mostly for entropic reasons.

Figure 3 shows the potential energy diagram for the reaction between acetylene and i-C_4H_5 radicals. Addition to the secondary C atom is characterized by a lower barrier (11.6 kcal/mol) and a more stable complex (D_0(**4**) = 27.2 kcal/mol) than the equivalent process involving the primary C atom (13.6 kcal/mol and D_0(**5**) = 11.0 kcal/mol). This is mostly due to the presence of a conjugated π system in the formation of the branched radical. Complex **4** has four conformer structures, which interconvert rapidly. These isomerizations occur on a time scale comparable to those corresponding to internal energy relaxations and are best treated as internal rotations. Complex **4** can form a five-membered ring with a relatively low barrier (12.2 kcal/mol), which eventually decomposes to fulvene and an H atom. Complex **5**, on the other hand, can also form a six-membered ring, but the barrier for this process (8.0 kcal/mol) is higher than that for forming a five-membered ring (2.0 kcal/mol).

B. Rate Coefficients for n-C_4H_5 + C_2H_2. There have been no direct measurements of the rate coefficient or product distribution of this reaction, so the data in the literature are all

TABLE 2: Fitting Parameters for Calculated Rate Coefficients[a] and Equilibrium Constants[b] of *n*-C_4H_5+C_2H_2

channel		*P*, atm	*A*	*B*	*C*	*D*	*E*	*F*	*T*, K
P1	H + benzene	0	5.31×10^{-08}	−1.11	4568				500−2500
		0.01	2.28×10^{-08}	−1.00	4477				
		0.025	4.88×10^{-08}	−1.09	4660				
		0.1	2.28×10^{-08}	−1.00	4478				
		1	2.30×10^{-08}	−1.00	4479				
		10	2.81×10^{-08}	−1.03	4513				
		100	2.74×10^{-08}	−1.01	4771				
P2	H + fulvene	0	3.28×10^{-09}	−0.80	4401				500−2500
		0.01	2.52×10^{-09}	−0.76	4412				
		0.025	2.52×10^{-09}	−0.76	4412				
		0.1	2.53×10^{-09}	−0.76	4413				
		1	7.68×10^{-09}	−0.89	4601				
		10	2.89×10^{-05}	−1.86	6232				
		100	2.05×10^{-04}	−2.00	8129				
P3	H + CHCCHCHCHCH$_2$	0	1.20×10^{-13}	0.89	9252				650−2500
		0.01	1.86×10^{-15}	1.39	8723				
		0.025	1.90×10^{-15}	1.39	8727				
		0.1	2.42×10^{-15}	1.36	8777				
		1	1.87×10^{-15}	1.39	8723				
		10	8.47×10^{-15}	1.21	9065				
		100	4.94×10^{-14}	1.03	9784				
C_6H_7	**1 + 2 + 3**	1	$4.74 \times 10^{+24}$	−12.29	7902	5.80×10^{-30}	4.01	−2574	500−2500
		10	$2.39 \times 10^{+20}$	−10.08	8905	$2.64 \times 10^{+20}$	−33.59	−63439	500−2000
		100	$7.69 \times 10^{+10}$	−6.68	8499	$3.99 \times 10^{+03}$	−25.14	−57252	500−1500
		∞	6.31×10^{-17}	1.62	2233				500−2500
R1→1	K^{eq}		3.54×10^{-11}		−20631				300−2500
R1→3	K^{eq}		3.76×10^{-14}		−46575				
R1→2	K^{eq}		7.35×10^{-13}		−33076				

[a] Bimolecular rate coefficients, $k(T) = AT^B \exp(-C/T) + DT^E \exp(-F/T)$. Units are cm^3 molecule^{-1} s^{-1} and K. [b] Pseudo-first-order equilibrium constants, $K^{eq}(T) = A \exp(-C/T)$. Units of *C* are K; K^{eq} is nondimensional.

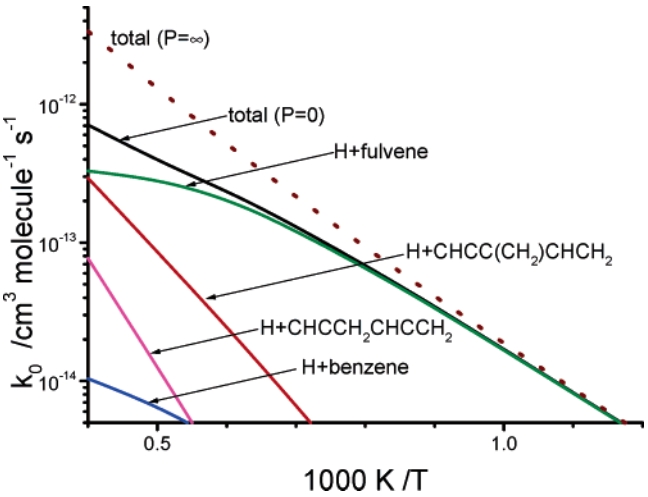

Figure 6. Arrhenius plot for the *i*-C_4H_5 + C_2H_2 reaction. The solid lines show the rate coefficients calculated at the collisionless limit for the total reaction and for the main product channels. The dotted line indicates the total rate coefficient at the high-pressure limit.

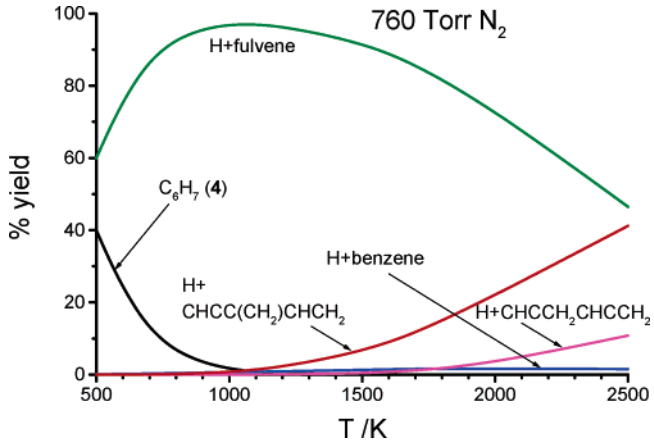

Figure 7. Product yields for the reaction of *i*-C_4H_5 with acetylene, calculated with 1 atm of N_2 bath gas.

derived from indirect determinations (or they are simply estimates). Most of these investigations attribute the reaction solely to the H + benzene channel. Some of this data[36−43] are shown in Figure 4, along with our calculations for this channel, performed for 1 atm of N_2 bath gas, and our total rate coefficients for the collisionless and the high-pressure limits. As evidenced by the small difference between these two limits, this reaction is relatvely insensitive to pressure.

Our calculations for the benzene channel are about 50% higher than the QRRK results of Westmoreland and co-workers[43] and the values estimated by Weissman and Benson[44] using group additivity methods. Most of the other previous studies report significantly smaller rate coefficients; the exceptions are the early shock-tube studies of Frenklach and co-workers,[38,39] in which significantly larger values for this rate coefficient were used. The relative product yields calculated as a function of temperature at 760 Torr of N_2 bath gas are shown in Figure 5. At 500 K, roughly 5% is stabilized as C_6H_7 molecules (corresponding mostly to compounds **2** and **3**). The strikingly small proportion of stabilization is a consequence of the small cyclization barriers (relative to the energy of the entrance channel) and the low-energy exit barriers of the subsequent decomposition steps. Benzene and fulvene products are produced roughly in a 2:1 ratio, which remains fairly constant at temperatures above 500 K because of the similar cyclization barriers. At high temperatures (≥1500 K), H-atom elimination from **1** becomes competitive despite the larger reaction barrier (38.9 kcal/mol) involved; this is due to the larger entropy of the transition state for H-atom elimination.

C. Rate Coefficients for *i*-C_4H_5 + C_2H_2. Calculated rate coefficients of the reaction of *i*-C_4H_5 with C_2H_2 in the collisionless limit are shown in Figure 6 for the total reaction

TABLE 3: Fitting Parameters for Calculated Rate Coefficients[a] and Equilibrium Constants[b] of *i*-C_4H_5+C_2H_2

channel		*P*, atm	*A*	*B*	*C*	*D*	*E*	*F*	*T*, K
P1	H + benzene	0	1.20×10^{-01}	−3.21	12397				800−2500
		0.01	2.44×10^{-01}	−3.28	12535				
		0.025	2.44×10^{-01}	−3.28	12535				
		0.1	2.44×10^{-01}	−3.28	12535				
		1	2.77×10^{-01}	−3.30	12561				
		10	$1.37 \times 10^{+01}$	−3.76	13368				
		100	$8.92 \times 10^{+08}$	−5.84	17626				
P2	H + fulvene	0	$1.26 \times 10^{+01}$	−3.46	10241				650−2500
		0.01	$1.08 \times 10^{+01}$	−3.44	10226				
		0.025	$1.67 \times 10^{+10}$	−5.94	14487				
		0.1	$1.08 \times 10^{+01}$	−3.44	10226				
		1	$1.13 \times 10^{+01}$	−3.45	10235				
		10	$1.61 \times 10^{+02}$	−3.76	10733				
		100	$8.67 \times 10^{+17}$	−7.94	19928				
P4	H + $CHCC(CH_2)CHCH_2$	0	5.66×10^{-06}	−1.37	15159				1000−2500
		0.01	9.28×10^{-06}	−1.43	15270				
		0.025	9.47×10^{-06}	−1.43	15275				
		0.1	1.21×10^{-05}	−1.46	15332				
		1	9.28×10^{-06}	−1.43	15270				
		10	9.33×10^{-05}	−1.69	15820				
		100	7.81×10^{-01}	−2.73	18189				
P5	H + $CHCCH_2CHCCH_2$	0	1.05×10^{-08}	−0.52	19336				1000−2500
		0.01	1.07×10^{-08}	−0.52	19345				
		0.025	1.07×10^{-08}	−0.52	19345				
		0.1	1.07×10^{-08}	−0.52	19345				
		1	1.10×10^{-08}	−0.53	19352				
		10	1.65×10^{-08}	−0.57	19450				
		100	9.42×10^{-07}	−1.04	20424				
C_6H_7	**4** + **7**	1	$1.90 \times 10^{+07}$	−9.21	9765	$7.21 \times 10^{+15}$	−9.12	9668	500−2000
		10	$1.11 \times 10^{+28}$	−11.97	14930	$5.98 \times 10^{+27}$	−28.03	−35507	
		100	$6.70 \times 10^{+18}$	−8.76	14504	$5.67 \times 10^{+17}$	−25.42	−39092	
	total	∞	2.21×10^{-17}	1.83	5892				500−2000
R2→5	K^{eq}		3.55×10^{-10}		−5862				300−2500
R2→4	K^{eq}		6.18×10^{-11}		−13624				
R2→7	K^{eq}		2.26×10^{-13}		−36081				
R2→6	K^{eq}		5.42×10^{-14}		−24345				

[a] Bimolecular rate coefficients, $k(T) = AT^B \exp(-C/T) + DT^E \exp(-F/T)$. Units are cm^3 $molecule^{-1}$ s^{-1} and K. [b] Pseudo-first-order equilibrium constants, $K^{eq}(T) = A \exp(-C/T)$. Units of *C* are K; K^{eq} is nondimensional.

and the individual bimolecular product channels. Also shown in this figure is the capture rate coefficient (k_∞), indicated with a dotted line. No data at all have been reported in the literature for this reaction despite its potential importance. Because of the higher addition barrier involved, the total rate coefficients are about one order of magnitude smaller (below 1200 K) than those of the reaction for *n*-C_4H_5 radicals. The main products of this reaction are fulvene and H atoms, as can be seen in Figure 7. The cyclization step is so fast that virtually all C_6H_7 stabilized corresponds to compound **7**, and only at high pressures (≥10 atm) does one begin to see the stabilization of another compound (**4**). However, compared with the reaction of *n*-C_4H_5 radicals, there is a larger proportion of C_6H_7 complexes stabilized, as the barrier for the cyclization of **4** is somewhat higher (12.2 kcal/mol). Again, at high temperatures (≥1500 K) H-atom elimination becomes competitive because of the large entropy of this reaction channel. For all temperatures and pressures studied, production of benzene from this reaction is insignificant (≤2%).

Although the barriers for isomerization of **5** are considerably smaller than those for **4**, addition to the terminal C atom of *i*-C_4H_5 radicals is relatively unimportant. For example, at 1000 K the capture rate coefficient for this channel is only 12% of the total value, and at 2000 K, this fraction is only 20%.

IV. Concluding Remarks

Unfortunately, there is a dearth of experimental information on the reactions that concern us in this article. Nevertheless, it is essential to have reliable rate coefficients for modeling. On the basis of our prior experience with the methods employed here, we believe that the present analysis provides such rate coefficients. Tables 2 and 3 give the rate coefficients as a function of temperature and pressure in a form that can be used in modeling.

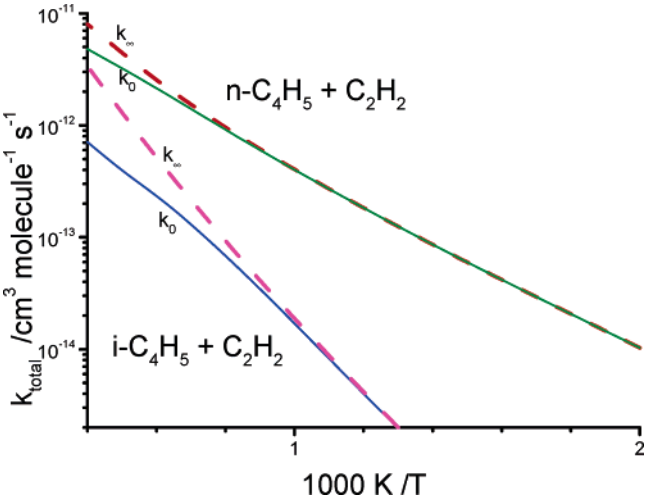

Figure 8. Arrhenius plot for C_2H_2 addition to *n*- and *i*-C_4H_5. The thin solid lines show rate coefficients calculated at the collisionless limit, while the dashed lines indicate results at the high-pressure limit.

Figure 8 shows that the rate coefficient for *n*-C_4H_5 + C_2H_2 is considerably larger than that for *i*-C_4H_5 + C_2H_2. However,

because the *n*- isomer is relatively easily converted to the *i*-form by H-atom-assisted isomerization in rich flames,[8] it is the *i*-C_4H_5 + C_2H_2 reaction that plays the more important role in flame chemistry. We have employed the rate coefficients reported here in some preliminary modeling of a series of low-pressure flames (acetylene, ethylene, allene, propyne, propene, and 1,3-butadiene) previously studied experimentally by others, all near the sooting limit. In the 1,3-butadiene flame,[45] *i*-C_4H_5 + C_2H_2 accounts for virtually all of the fulvene produced in the flame and indirectly through the H-assisted isomerization of fulvene to benzene,[3] perhaps as much as 30% of the benzene. The remainder, of course, comes primarily from the C_3H_3 + C_3H_3 recombination. The contributions of *i*-C_4H_5+C_2H_2 are considerably less in the other flames, and the contributions of *n*-C_4H_5 + C_2H_2 to forming cyclic products are largely negligible in all of the flames. However, one should not be too quick to generalize these conclusions. Practical fuels normally involve larger molecules than the ones we have considered. In such cases, *i*-C_4H_5 (or 1,3-butadiene as a precursor) may be formed from breaking down larger molecules, perhaps resulting in relatively larger concentrations than can be formed from the building up process required in the flames we have investigated (except for the 1,3-butadiene flame, of course). The *i*-C_4H_5 + C_2H_2 reaction may be more important under such conditions.

Acknowledgment. This work has been supported by the United States Department of Energy, Office of Basic Sciences, Division of Chemical Sciences, Geosciences and Biosciences. Sandia is a multiprogram laboratory operated by Sandia Corporation, a Lockheed Martin Company, for the United States Department of Energy's National Nuclear Security Administration under Contract No. DE-AC04-94AL85000. J.P.S. would like to thank the European Research and Training Network NANOQUANT, Contract No. MRTN-CT-2003-506842, for financial support.

Supporting Information Available: Rovibrational properties of isomers, saddlepoints and bimolecular products, and parametric fits of potentials for internal rotations, calculated using the uB3LYP/6-311++G(d,p) model chemistry. This information is available free of charge via the Internet at http://pubs.acs.org.

References and Notes

(1) Miller, J. A. *Symp. (Int.) Combust., [Proc.]* **1996**, *26*, 461.
(2) Miller, J. A. *Faraday Discuss.* **2001**, *119*, 461.
(3) Miller, J. A.; Pilling, M. J.; Troe, J. *Proc. Combust. Inst.* **2005**, *30*, 43.
(4) Richter, H.; Howard, J. B. *Prog. Energy Combust. Sci.* **2000**, *26*, 565.
(5) Glassman, I. *Symp. (Int.) Combust., [Proc.]* **1989**, *22*, 295.
(6) McEnally, C. S.; Lisa, D. P.; Burak, A.; Kohse-Hoinghaus, K. *Prog. Energy Combust. Sci.* **2006**, *32*, 247.
(7) Miller, J. A.; Klippenstein, S. J. *J. Phys. Chem. A* **2003**, *107*, 7783.
(8) Miller, J. A.; Melius, C. F. *Combust. Flame* **1992**, *91*, 21.
(9) Hansen, N.; Klippenstein, S. J.; Taatjes, C. A.; Miller, J. A.; Wang, J.; Cool, T. A.; Yang, B.; Yang, R.; Wei, L. X.; Huang, C. Q.; Qi, F.; Law, M. E.; Westmoreland, P. R. *J. Phys. Chem. A* **2006**, *110*, 3670.
(10) Miller, J. A.; Klippenstein, S. J. *J. Phys. Chem. A* **2003**, *107*, 2680.
(11) Miller, J. A.; Klippenstein, S. J.; Robertson, S. H. *J. Phys. Chem. A* **2000**, *104*, 7525. See also *J. Phys. Chem. A* **2000**, *104*, 9806−9806 (correction).
(12) Becke, A. *Phys. Rev. A* **1988**, *38*, 3098.
(13) Stephens, P. J.; Devlin, F. J.; Chabalowski, C. F.; Frisch, M. J. *J. Phys. Chem.* **1994**, *98*, 11623.
(14) Baboul, A. G.; Schlegel, H. B. *J. Chem. Phys.* **1997**, *107*, 9413.
(15) Hampel, C.; Peterson, K. A.; Werner, H.-J. *Chem. Phys. Lett.* **1992**, *190*, 1.
(16) Amös, R. D.; Andrews, J. S.; Handy, N. C.; Knowles, P. J. *Chem. Phys. Lett.* **1991**, *185*, 256.
(17) For details see *Proc. Combust. Inst.* **2007**, doi:10.1016/j.proci.2006.08.084 (in press).
(18) Mayer, P. M.; Parkinson, C. J.; Smith, D. M.; Radom, L. *J. Chem. Phys.* **1998**, *108*, 604.
(19) Senosiain, J. P.; Fernández, B.; Miller, J. A., in preparation.
(20) Frisch, M. J.; Trucks, G. W.; Schlegel, H. B.; Scuseria, G. E.; Robb, M. A.; Cheeseman, J. R.; Montgomery, J. A., Jr.; Vreven, T.; Kudin, K. N.; Burant, J. C.; Millam, J. M.; Iyengar, S. S.; Tomasi, J.; Barone, V.; Mennucci, B.; Cossi, M.; Scalmani, G.; Rega, N.; Petersson, G. A.; Nakatsuji, H.; Hada, M.; Ehara, M.; Toyota, K.; Fukuda, R.; Hasegawa, J.; Ishida, M.; Nakajima, T.; Honda, Y.; Kitao, O.; Nakai, H.; Klene, M.; Li, X.; Knox, J. E.; Hratchian, H. P.; Cross, J. B.; Bakken, V.; Adamo, C.; Jaramillo, J.; Gomperts, R.; Stratmann, R. E.; Yazyev, O.; Austin, A. J.; Cammi, R.; Pomelli, C.; Ochterski, J. W.; Ayala, P. Y.; Morokuma, K.; Voth, G. A.; Salvador, P.; Dannenberg, J. J.; Zakrzewski, V. G.; Dapprich, S.; Daniels, A. D.; Strain, M. C.; Farkas, O.; Malick, D. K.; Rabuck, A. D.; Raghavachari, K.; Foresman, J. B.; Ortiz, J. V.; Cui, Q.; Baboul, A. G.; Clifford, S.; Cioslowski, J.; Stefanov, B. B.; Liu, G.; Liashenko, A.; Piskorz, P.; Komaromi, I.; Martin, R. L.; Fox, D. J.; Keith, T.; Al-Laham, M. A.; Peng, C. Y.; Nanayakkara, A.; Challacombe, M.; Gill, P. M. W.; Johnson, B.; Chen, W.; Wong, M. W.; Gonzalez, C.; Pople, J. A. *Gaussian 03*, revision C.02; Gaussian, Inc.: Wallingford, CT, 2004.
(21) Werner, H.-J.; Knowles, P. J.; Amös, R. D.; Bernhardsson, A.; Berning, A.; Celani, P.; Cooper, D. L.; Deegan, M. J. O.; Doobbyn, A. J.; Eckert, F.; Hampel, C.; Hetzer, G.; Korona, T.; Lindh, R.; Lloyd, A. W.; McNicholas, S. J.; Manby, F. R.; Meyer, W.; Mura, M. E.; Nicklass, A.; Palmieri, P.; Pitzer, R.; Rauhut, G.; Schütz, M.; Schumann, U.; Stroll, H.; Stone, A. J.; Tarroni, R.; Thorsteinsson, T. MOLPRO is a package of ab initio programs; version 2002.1, 1998.
(22) Pitzer, K. S.; Gwinn, W. D. *J. Chem. Phys.* **1942**, *10*, 428.
(23) Senosiain, J. P.; Miller, J. A.; Klippenstein, S. J. *J. Phys. Chem. A* **2005**, *109*, 6045.
(24) Reith, D. Thermal Diffusion in Binary Lennard-Jones Liquids. diploma thesis, Universit Mainz, 1998.
(25) Hold, U.; Lenzer, T.; Luther, K.; Reihs, K.; Symonds, A. *Ber. Bunsen.-Ges. Phys. Chem.* **1997**, *101*, 552.
(26) Klippenstein, S. J.; Miller, J. A. *J. Phys. Chem. A* **2002**, *106*, 9267.
(27) Hahn, D. K.; Klippenstein, S. J.; Miller, J. A. *Faraday Discuss.* **2001**, *119*, 79.
(28) Miller, J. A.; Klippenstein, S. J. *J. Phys. Chem. A* **2006**, *110*, 10528.
(29) Miller, J. A.; Parrish, C.; Brown, N. J. *J. Phys. Chem.* **1986**, *90*, 3339.
(30) Klippenstein, S. J.; Wagner, A. F.; Dunbar, R. C.; Wardlaw, D. M.; Robertson, S. H.; Miller, J. A. *VARIFLEX;* 1.13m ed., 2003.
(31) Wheeler, S. E.; Allen, W. D.; Schaefer, H. F. *J. Chem. Phys.* **2004**, *121*, 8800.
(32) Also called the IRCmax. See Malick, D. K.; Petersson, G. A.; Montgomery, J. A. *J. Chem. Phys.* **1998**, *108*, 5704.
(33) Small differences in the positions of the maxima computed with uB3LYP and higher levels of theory are partly accounted for by the variational treatment of the addition channels.
(34) Lee, T. J.; Rendell, A. P.; Taylor, P. R. *J. Phys. Chem.* **1990**, *94*, 5463.
(35) Lee, T. J.; Taylor, P. R. A diagnostic for determining the quality of single-reference electron correlation methods. Presented at the International Symposium on Quantum Chemistry, Solid-State Theory and Molecular Dynamics, St. Augustine, FL, 1989.
(36) Cole, J. A.; Bittner, J. D.; Longwell, J. P.; Howard, J. B. *Combust. Flame* **1984**, *56*, 51.
(37) Colket, M. B. *Symp. (Int.) Combust., [Proc.]* **1986**, *21*, 851.
(38) Frenklach, M.; Clary, D.; Gardiner, W. C. J.; Stein, S. E. *Symp. (Int.) Combust., [Proc.]* **1984**, *20*, 887.
(39) Frenklach, M.; Warnatz, J. *Combust. Sci. Tech.* **1987**, *51*, 265.
(40) Harris, S. J.; Weiner, A. M.; Blint, R. J. *Combust. Flame* **1988**, *72*, 91.
(41) Kern, R. D.; Singh, H. J.; Wu, C. H. *Int. J. Chem. Kinet.* **1988**, *20*, 731.
(42) Wang, H.; Frenklach, M. *J. Phys. Chem.* **1994**, *98*, 11465.
(43) Westmoreland, P. R.; Dean, A. M.; Howard, J. B.; Longwell, J. P. *J. Phys. Chem.* **1989**, *93*, 8171.
(44) Weissman, M. A.; Benson, S. W. *J. Phys. Chem.* **1988**, *92*, 4080.
(45) Unpublished work.
(46) Colket, M. B.; Seery, D. J.; Palmer, H. B. *Combust. Flame* **1989**, *75*, 343.